# All-Analogue Real-Time Broadband Filter Bank Multicarrier Optical Communications System

Fernando A. Gutiérrez, Philip Perry, *Member, IEEE,* Eamonn P. Martin, Andrew D. Ellis, *Member, IEEE,* Frank Smyth, *Member, IEEE,* and Liam P. Barry, *Senior Member, IEEE.*

*Abstract*— **This paper studies the key aspects of an optical link which transmits a broadband microwave filter bank multicarrier (FBMC) signal. The work is presented in the context of creating an all-analogue real-time multi-gigabit orthogonal frequency division multiplexing (OFDM) electro-optical transceiver for short range and high capacity data center networks. Passive microwave filters are used to perform the pulse shaping of the bit streams, allowing an orthogonal transmission without the necessity of digital signal processing (DSP). Accordingly, a cyclic prefix that would cause a reduction in the net data rate is not required. An experiment consisting of three orthogonally spaced 2.7 Gbaud quadrature phase shift keyed (QPSK) subchannels demonstrates that the spectral efficiency of traditional DSP-less subcarrier multiplexed (SCM) links can be potentially doubled. A sensitivity of -29.5 dBm is achieved in a 1 kilometer link.**

*Index Terms*— **Electro optical transceiver, Filter Bank Multicarrier (FBMC), Orthogonal Frequency Division Multiplexing (OFDM), Subcarrier Multiplexing (SCM).**

## I. INTRODUCTION

THE increasing demand for capacity in optical links has motivated the development of more spectrally efficient transmission schemes during the last few decades. More recently, the proliferation of data centers has stimulated a growing research effort in optical interconnects and its associated technologies [1]. Digital multicarrier techniques have been thoroughly explored as they can divide the available transmission bandwidth into narrower-band radio frequency (RF) and optical subsystems that can be processed independently. Although all-optical multicarrier schemes have proven to be valid for real-time implementations [2], they are still complex and require stable coherent optical frequency combs. For more practical and industrial applications, electrical and microwave components are preferred because of the maturity and stability that they present, in contrast with their optical counterparts. Consequently, wavelength division multiplexing (WDM) schemes have been implemented employing electrical subsystems in the transmitter and/or the receiver, as in coherent WDM [3] or Nyquist WDM [4]. However, to decrease the number of total optical wavelengths, these systems require broadband baseband signals of tens of Gbaud, which limits its performance and increases the cost and difficulty of any practical real-time implementation. Subcarrier multiplexing (SCM) is a different alternative that combines several RF subchannels into one signal, which is then modulated onto an optical wavelength before transmission over fiber. Thus, WDM/SCM systems present the advantage of employing microwave components with narrower baseband signals [5].

SCM has been employed in many implementations. Early SCM systems were used to transmit a number of low bandwidth video signals [6]. Later on, and in line with present requirements, frequency plans with a smaller number of broadband subchannels were reported [7, 8]. Currently, the advances in high-speed analog-to-digital and digital-to-analog converters (ADC, DAC) have motivated the implementation of SCM schemes with hybrid analogue-digital processing [9, 10]. Most importantly, spectral efficiency can be maximized by transmitting multiple orthogonally overlapping subchannels, like in orthogonal frequency division multiplexing (OFDM) [11]. However, the implementation of real-time broadband OFDM schemes requires demanding and complicated digital signal processing (DSP) techniques [12]. In intensive DSP based systems, the main disadvantages are the associated high power consumptions [13] and often latencies. Depending on their size and their targeted market, different subsystems inside optical networks can present totally dissimilar requirements of spectral efficiency, power consumption, and latency. A purely analogue orthogonal SCM (OSCM) system potentially offers the best trade-off between those key parameters in certain real-time applications.

It can be concluded that traditional broadband SCM is a reliable technique, whose main weakness in spectral efficiency can be eliminated if orthogonally overlapping subchannels are employed. The previous discussion motivates the search and the analysis of an all-analogue OSCM implementation, as a means to achieve DSP-less broadband OFDM optical links. A similar concept was simulated in [14]. More recent results have demonstrated the capabilities of the technique in a WDM system employing an optical comb based transmitter [15], but
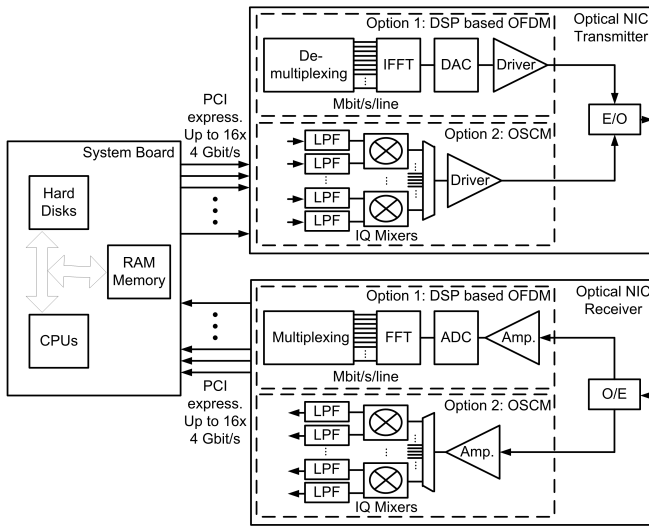
Fig. 1. Optical NIC showing two different options for an orthogonal transmission: FFT-based OFDM and OSCM.

a detailed description and analysis of the basic OSCM system has not been provided. This manuscript demonstrates and thoroughly investigates how broadband SCM schemes can be implemented with orthogonally overlapping subchannels without requiring DSP. This is achieved by relying on the excellent stability and low phase noise of microwave oscillators, the frequency selectivity of microwave filters, and the good performance of inexpensive integrated microwave modulators. To validate the proposed concept, an optical link consisting of three orthogonal 2.7 Gbaud quadrature phase shift keyed (QPSK) subchannels is employed, with the middle subchannel representing the worst case scenario with maximum interference. In the experiment, passive microwave filters are used to shape the multi-gigabit baseband data streams as Nyquist pulses, which enables the orthogonal modulation and demodulation of the subchannels. Moreover, the rate of 2.7 Gbaud is selected because it is compatible with interfaces between computers and network interface cards (NIC).

The rest of the text is organized as follows. Section II compares the integration of OSCM and DSP-based OFDM in optical NICs. Section III explores the key theoretical and practical concepts involved in OSCM links, from three different perspectives: the basic communication scheme (section III.A), the key microwave components (section III.B), and the optical configuration and parameters (section III.C). Section IV describes the experimental scheme and results obtained with a 1 km optical link. Finally, section V reviews the main conclusions of the presented work. Note that in this section, and in the remainder of the text, the terms component, subcarrier and subchannel are not ambiguous: the in-phase (I) and quadrature (Q) baseband components modulate one subcarrier producing one subchannel.

## II. OFDM OPTICAL NICS

Traditional DSP-based OFDM has been proposed for short reach optical networks, including in-building networks, access networks, mobile back-haul/front-haul and data centers [16].

Fig. 1 illustrates an optical NIC comparing two different implementations: DSP-based OFDM and OSCM. The interface between a computing system and the NIC is called "peripheral component interconnect express" (PCI express), which currently supports up to 16 digital lines with peak data rates of 4 Gbit/s per line [17].

OFDM, as shown in Fig. 1, requires the computation of the standard and the inverse fast Fourier transforms (FFT and IFFT). Those operations are complicated and integrated circuits need to parallelize the incoming data to reduce the rate per line from Gbit/s to Mbit/s in the transmitter [18]. Equivalently, the opposite multiplexing, from Mbit/s to Gbit/s, is required in the receiver. High-speed DACs and ADCs are necessary to achieve high transmission rates. Finally, a data driver and an amplifier are required in the transmitter and the receiver before the electro-optic and the opto-electronic converters (E/O and O/E). The use of narrowband subchannels is an advantage to compensate high values of accumulated fiber dispersion in long-haul optical communications systems [19], but the implementation of the (I)FFT in short reach systems might be justified only when spectral efficiency has to be maximized regardless of any penalty in resource demand and additional complexity [20]. Even for low modulation orders, there are three limitations in these implementations that cannot be avoided. Firstly, due to the (I)FFT based operation, a small amount of dispersion between two subcarriers affects the timing of consecutive symbols, impairing all the subchannels. As a result, a cyclic prefix (CP) that reduces the net rate is required for the transmission in any dispersive channel [11, 21]. Secondly, the power consumption increases due to the data interfaces and the ADCs and DACs [22]. Finally, a high number of subchannels translates into a very high peak to average power ratio (PAPR), with the corresponding penalty in the dynamic range and the power consumption [23].

In contrast, OSCM can potentially enable a simpler orthogonal implementation with several advantages. Fig. 1 shows the typical components of a broadband SCM system [8]. Baseband data can be directly processed with a low pass filter (LPF) and then used to modulate an RF subcarrier. All the subchannels are combined and multiplexed in a single signal that is amplified and fed to an E/O module. The opposite processing takes place in the receiver. The following section shows the particular conditions that must be met to employ orthogonal subchannels with this analogue implementation, but several advantages can already be deduced. As the number of subchannels is lower, so is the PAPR. No DSP, ADC's, DAC's, or demanding algorithms are required, which emphasizes the low power consumption. As only analogue components are used, latency is reduced to a minimum. In OSCM, unlike FFT-based OFDM, the dispersion suffered by one subcarrier only impairs the adjacent subchannels, so that the absence of a CP maximizes the data rate while the penalty in performance is negligible for short transmission distances. Moreover, the baseband incoming signals have a data rate that is directly compatible with broadband RF IQ mixers [24], avoiding data rate changes and
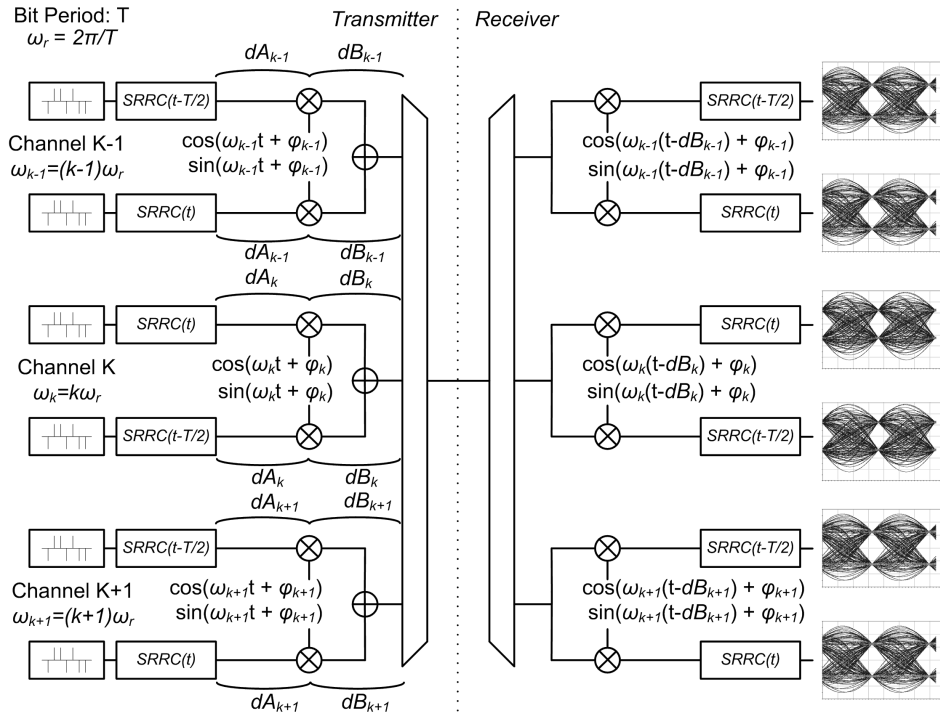
Fig. 2. Back to back FBMC scheme with three orthogonal QAM subchannels and arbitrary delays in every RF band at the transmitter.

interfaces. The system architecture used here is based largely on amplifiers and IQ Mixers, allowing an integrated low cost low power implementation with monolithic microwave integrated circuit (MMIC) technology [10, 25].

## III. FILTER BANK MULTICARRIER FOR MICROWAVE AND ELECTRO-OPTICAL APPLICATIONS

There are two methods that can be employed for the transmission of orthogonally spaced RF subcarriers: the Fourier transform, as in OFDM, or the use of the appropriate baseband filters at the transmitter and the receiver, as in filter bank multicarrier (FBMC) [26, 27]. FBMC permits a simpler implementation with only analogue components and was employed in this work. Orthogonal quadrature amplitude modulated (QAM) transmission can be accomplished when the following three conditions are met [26, 27]. Firstly, every pair of baseband data streams, which will modulate a particular subcarrier, must present a relative time delay equal to half a bit period. Secondly, the delayed and non-delayed baseband data streams that form a pair must act as the in-phase and the quadrature components alternatively in different subcarriers. Finally, the baseband digital data streams at the transmitter must be filtered in order that every bit has the shape of a square root raised cosine (SRRC) pulse, and the baseband filter at the receiver must present the matched SRRC response. When these conditions are ensured, each received baseband signal will present a sampling point in the middle of the bit period that is free of inter symbol and inter channel interference (ISI and ICI). The following subsections analyze the key concepts involved in the design of a broadband OSCM electro-optical transceiver based on FBMC theory.

### A. Theoretical Microwave FBMC Communications Scheme

Fig. 2 shows a three subcarrier FBMC scheme where the bit period is $T$, the angular data frequency is $\omega_r$, and the conditions described at the beginning of section III can be observed. Additionally, the delays that can be found in the transmitter, in any real microwave implementation, are also included. For the $i^{th}$ frequency band, where $i$ is an integer that can present three consecutive values ($k-1$, $k$, $k+1$) and the subcarrier frequency is $i \cdot \omega_r$: the term $dA_i$ accounts for any delay of the baseband pair prior to the IQ mixing, $dB_i$ represents the delay after the mixing and before the overall combination of subchannels, and $\varphi_i$ is the phase shift in the LO with respect to the ideal case. The LOs at the receiver in Fig. 2 are locked to the incoming signal, as in any FDM transmission system. Without losing generality, the delays in the channel or in the receiver have not been included.

When all the delays ($dA_i$, $dB_i$, and $\varphi_i$) are zero, as in an ideal case or in a completely digital implementation, the received eye diagrams are free of ISI and ICI, as can be observed in the simulated results shown in Fig. 2. Since the central subchannel has more interfering neighbors than the others, the phase margin of its associated eye diagram is reduced, while still remaining perfectly open at the sampling instant. The number of subchannels could be extended to any practical number resulting in equivalent eye diagrams for the extreme and intermediate subchannels, presenting an optimum sample point free of ISI and ICI. In any practical implementation, different IQ mixers will present different values of $dA_i$ and $dB_i$. Despite these impairments, perfect system functionality, with a sampling instant free of ISI and ICI, can be achieved by adjusting only the phases of the LOs $\varphi_i$ according to the values derived in the Appendix at the end of text (eq. (8) and (9)).

It can be concluded that, in a real implementation, the phases in the transmitter can be adjusted by simply inserting appropriate fixed delays in the baseband signals (*T/2* shift inside each pair) and in the LOs. In the receiver, the LOs have to be locked to the phase of the incoming signal, as in any SCM link. This can be accomplished with pilot tones plus phase locked loops (PLL) [28]. As all the LOs are orthogonal, the synchronization can be simplified using a single pilot tone plus PLLs [29, 30], or, potentially, a single PLL plus an electrical comb. In the bench experiments presented in section IV, variable phase shifters were used in the LOs of the transmitter and the receiver to obtain maximum flexibility.

*B. Microwave Orthogonality Filters*

A broadband purely analogue implementation of the scheme presented in Fig. 2 requires multi-gigabit baseband signals shaped as SRRC and ideal microwave SRRC filters. Three main difficulties must be solved. Firstly, the original sourced bits are square signals, instead of impulses, with a sinc spectrum. The baseband filters in the transmitter must compensate the sinc input to obtain the SRRC shape at its output. Secondly, as the performance of the system is based in the pulse shape of every bit, it is important to ensure that quasi-square signals arrive to the input of this orthogonality filters in the transmitter. Although the attenuation of high frequency components is common in any circuit, these effects can be compensated using pre-emphasis in the analogue source. The new block diagram of the baseband transmitter for one RF band incorporating the two previous concepts can be observed in Fig. 3. Finally, microwave SRRC filters require a sharp roll-off and constant group delay, but both features are not compatible using standard microwave filter design techniques [31], and, therefore, delay equalizers are required. Common low pass filter topologies can also be used, although with limited performance [14]. For this work, pseudo ideal SRRC filters were designed as they obtain much narrower frequency outputs, relaxing the specifications required for the IQ mixers, and as a starting point in the design of quasi-ideal microwave orthogonality filters.

The bandwidth of an SRRC filter (and a sinc compensated SRRC filter) depends on the beta factor ($\beta$), which can vary from zero to one. If the bitrate of the baseband data is $f_r$, the
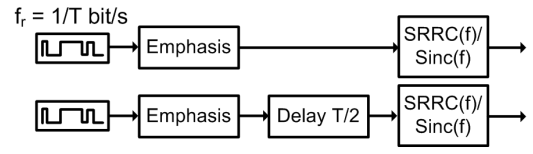


Fig. 3. All-analogue baseband transmitter, including the two components that modulate one subcarrier.

frequency response of the associated SRRC filter extends from DC to the following frequency $f_{BW}=0.5 \cdot f_r(1+\beta)$. Regardless of the value of $\beta$, perfect system functionality is obtained in FBMC. However, restrictions arise due to limitations in a microwave implementation. If $\beta$ was very low, the filter would be very abrupt, making it more difficult to compensate group delay. If $\beta$ was very high, the compensation of the sinc response at the transmitter would be more difficult because the sinc function at $f_r$ is equal to zero. For this work, microwave *SRRC(f)* and *SRRC(f)/Sinc(f)* filters were designed for a rate of 2.7 Gbps. In practice, during the filter design process, a value of $\beta=0.5$ was found to be suitable, as it was conducive to physically realizable filters with almost perfect frequency response, while the impairments in the group delay did not compromise the achievable eye diagrams. Fig. 4 shows the frequency response and the group delay of the developed filters, and compares them with ideal implementations. The microwave FBMC system was simulated including: the achieved *SRRC(f)/Sinc(f)* filters in the transmitter, the achieved *SRRC(f)* filters in the receiver, perfect square signals in the data source, and, finally, ideal devices for the rest of the components (IQ mixers, power combiners and splitters). The received eye diagram obtained for one component allocated in an intermediate subcarrier can also be observed in Fig. 4.

*C. Optical Link*

The configuration of the microwave FBMC transmitter and receiver has been explained in the previous subsections. The electrical signal generated in the transmitter must be modulated onto an optical carrier. An optical single side band signal (SSB) is preferred as it allows a WDM implementation with closer optical channel spacing [5], achieving a higher spectral efficiency. Dual-drive Mach-Zehnder modulators (DD-MZM) and optical IQ modulators (OIQM) can achieve optical SSB directly, without requiring additional optical
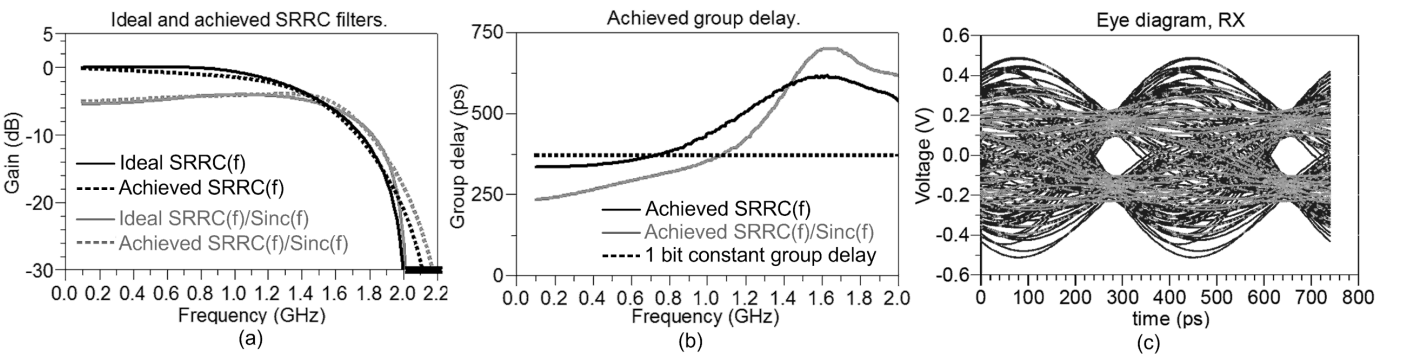


Fig. 4. Ideal and achieved performance of passive microwave SRRC filters for a rate of 2.7 Gbps where $\beta=0.5$ with and without sinc compensation: (a) amplitude response and (b) group delay compared with an ideal case where it is constant and equal to 1 bit interval. (c) Simulated received eye diagram, in a back to back microwave FBMC scheme, for an intermediate subchannel, when the achieved sinc compensated SRRC filters are employed in the transmitter and the achieved SRRC filters are employed in the receiver.
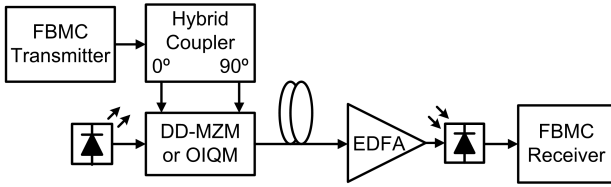
Fig. 5. Block diagram of an OSCM/SSB link with a pre-amplified optical receiver.

filters [32, 33]. The block diagram of a direct detection (DD) OSCM/SSB scheme with a pre-amplified optical receiver is illustrated in Fig. 5. The optical modulator has two electrical inputs; one needs to be fed with the desired microwave signal, and the other with its Hilbert transform (HT) (the original signal with all the frequencies shifted 90 degrees). In the analogue domain, the HT is obtained with a microwave 90 degrees hybrid coupler.

The theory of multicarrier links based on optical modulators has been extensively studied. For short transmission distances, the sensitivity of the link can be analyzed as a function of the optical modulation index (OMI), the bias point in the modulator, the optical carrier suppression and the bandwidth of the baseband signals; as it was done in [34, 35] for the DD-MZM and in [36] for the OIQM. The previous studies are directly applicable to OSCM when the optical noise generated in the receiver is the dominant impairment determining the sensitivity of the link. The optical link that will be presented in the experimental section was numerically analyzed. An OSCM/SSB link based on an OIQM biased at *quadrature* was considered. The frequency plan consisted of three 2.7 Gbaud QPSK orthogonal subchannels, located at the second, third, and fourth harmonics of the data rate. According to [36], for a bit error rate (BER) of $3.8\cdot10^{-3}$ (quality factor $Q_F$=2.67), sensitivities of -32.4 dBm and -31 dBm are theoretically achievable with SRRC pulses of $\beta$=0.1 and $\beta$=0.5 respectively. Previous results were obtained with an overall rms OMI of 21% with respect to $V_\pi$ and considering a pre-amplified optical receiver whose Erbium doped fiber amplifier (EDFA) presents a noise figure of 5 dB. The described system was simulated using the simulation software VPI. Sensitivity was obtained

for the middle subchannel as a function of the phase error in the receiver LO. Fig. 6 shows the obtained results. A lower value of $\beta$ reduces the bandwidth of the data and makes it more tolerant to the noise in the receiver achieving better sensitivity. The sensitivities for the case of perfect synchronization (no phase error) are similar to the previous predictions. According to [27], there is a margin of $\approx \pm7.5$ degrees in the subcarrier phase offset in the receiver with associated peak power distortions below 3 dB. As those are peak distortions and the sensitivity of the system represents an average power, the influence of the subcarrier phase error on system performance can be lower than the previous estimation.

When transmitting over fiber, dispersion can affect the orthogonality that is established in the transmitter (as described in section III.A). The distortion generated in the received signals, due to dispersive media in FBMC links, was theoretically analyzed in [27]. When SRRC shapes with $\beta$=0.5 are used, the distortion per km, $\gamma$, measured as a percentage of the absolute value of the desired received signal is [27]:

$$\gamma = 1.1\cdot\frac{D}{T^2}\cdot100 \quad (\%/km) \tag{1}$$

where $D$ is the dispersion of the channel in (s/Hz)/km. The dispersion of standard single mode fiber (SSMF) is 17 (ps/nm)/km at 1550 nm [37], being $D\approx1.3614\cdot10^{-22}$ (s/Hz)/km. From eq.(1), and considering a rate of 2.7 Gbaud, the distortion in a received FBMC signal transmitted through SSMF is $\gamma \approx 0.1$ %/km. It can be concluded that the effect of dispersion in short range OSCM links over SSMF is negligible. The experimental results described in section IV present a good agreement with the theoretical predictions.

The work presented in this manuscript is focused on short reach links, but OSCM/SSB is also suitable for longer transmission distances according to the following perspectives. Firstly, SSB was originally developed as a method to overcome dispersive fading [32, 38]. With that technique, SCM/SSB signals have been transmitted over hundreds of km with no penalty due to chromatic dispersion [39]. Secondly, several independent studies have concluded that the optimum subcarrier spacing for long transmission distance over SSMF is within the range of 2-10 Gbaud [40-43]. While that spacing is prohibitive for single-carrier dense WDM links, it is ideal for WDM/SCM or WDM/OSCM, as closer electrical subchannels can be allocated in the electrical domain with a lower cost and complexity. Finally, according to eq. (1), the penalty generated by fiber dispersion is small in OSCM even for long transmission distances. In the calculated example, with a rate of 2.7 Gbaud, the distortion after 100 km of SSMF fiber would be $\approx$10 %. An analogy can be made with coherent WDM, where orthogonally overlapping subchannels are also multiplexed adjusting the phases at the transmitter [44], and dispersion penalties are small even for high speed rates transmitted over tens of km. [45].
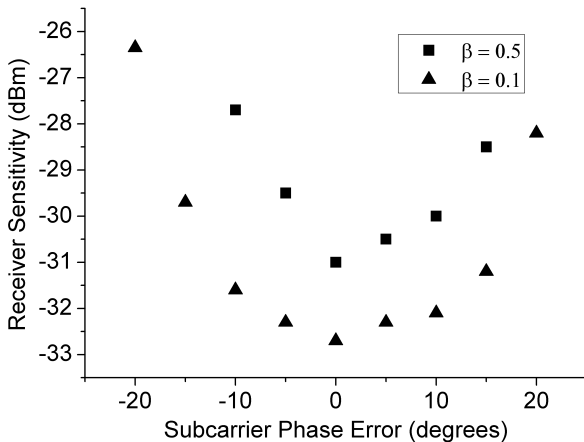


Fig. 6. Simulation of a back to back three subcarrier 2.7 Gbaud QPSK OSCM system based on an OIQM and a pre-amplified optical receiver. Sensitivities for $Q_F$=2.67 for different values of $\beta$ and as a function of phase error in the receiver LO of the middle subchannel.
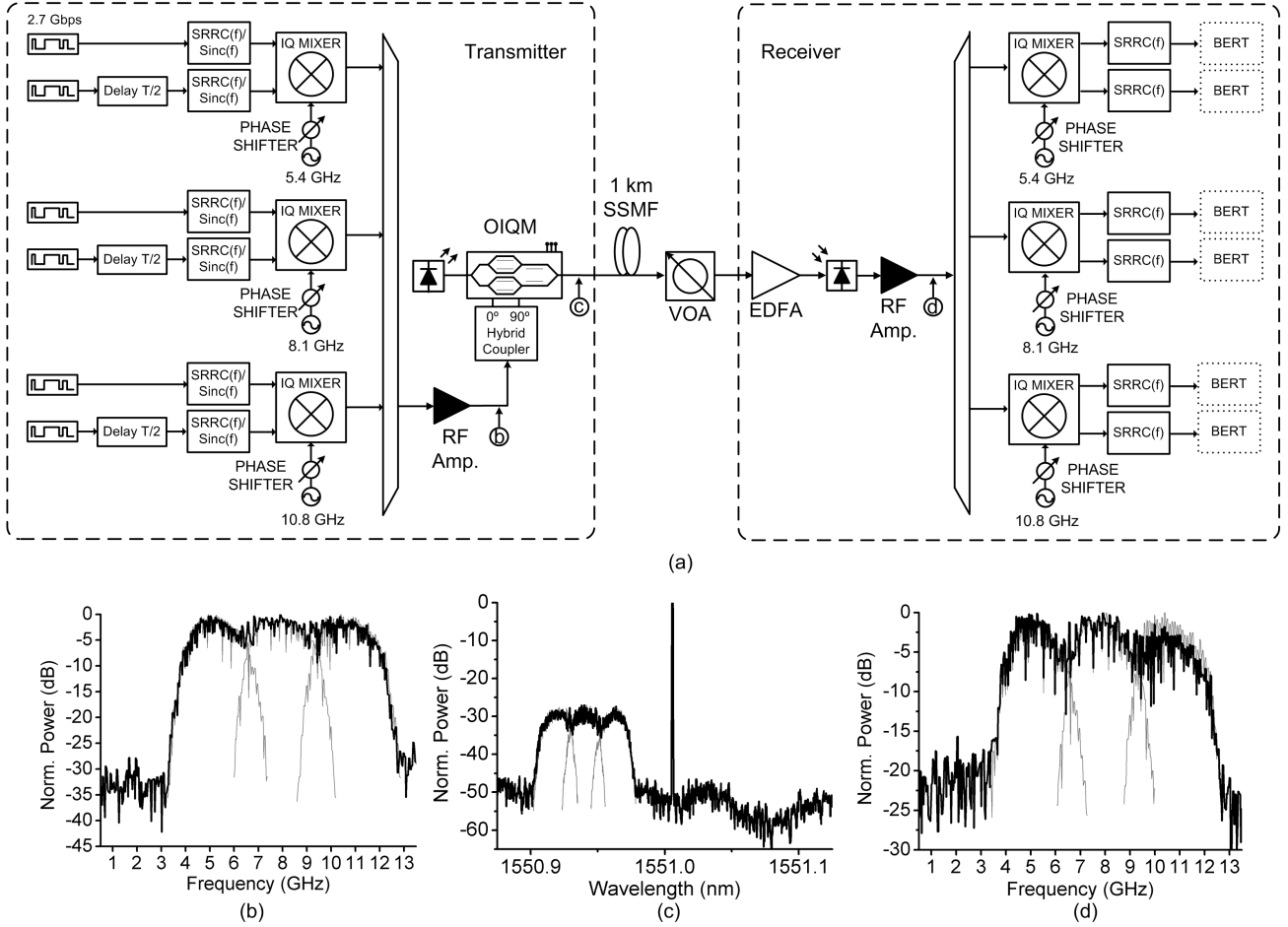
Fig. 7. (a) DD OSCM/SSB link consisting of three orthogonal 2.7 Gbaud QPSK subcarriers. Optical and electrical spectra are shown at: (b) the output of the RF FBMC transmitter, (c) the output of the optical modulator (resolution 180 MHz), and (d) the output of the photo-receiver. In all the spectra, the black line shows the overall spectrum, while the gray lines show individual subchannels measured when they are transmitted alone.

## IV. EXPERIMENTS

This section describes the physical link that was implemented to prove the feasibility of broadband OSCM, emphasizing the main ideas and concepts that have been explained in section III.

### A. Experimental Setup

The OSCM/SSB experimental setup is equivalent to that shown in Fig. 7(a). Inexpensive off-the-shelf MMIC IQ mixers were used to generate and demodulate a signal composed of three orthogonal QPSK subchannels modulated at 2.7 Gbaud. A master reference of 2.7 GHz was fed to the input of an electrical comb generator that provided the orthogonal LOs. A microwave filter was used to demultiplex the desired tones, namely the second, third and fourth harmonics of the data rate (5.4, 8.1 and 10.8 GHz). With the described frequency plan, the overall data rate was 16.2 Gbps over a bandwidth of 12.8 GHz (1.265 bit/s/Hz) including the optical carrier or 9.4 GHz (1.72 bit/s/Hz) excluding the optical carrier.

The FBMC transmitter was designed as follows. Six uncorrelated bit streams were sourced from a field programmable gate-array (FPGA) with integrated analogue transceivers. The FPGA data clock was frequency locked to the master reference. Pseudo random binary sequences (PRBS) of $2^{15}$-1 bits were used. In every pair of baseband signals, a $T/2$ relative phase shift was introduced using adjustable phase trimmers. Subsequently, both signals were pulse shaped with the sinc compensated SRRC filters, and, finally, connected to the baseband input ports of the IQ mixers. As explained in section III.B, the best performance was obtained when quasi-square signals arrived to the input of the orthogonality filters. This was achieved using the emphasis functionality that modern FPGAs incorporate in the analogue transceivers [46]. The phases of the LOs that feed the IQ mixers were adjusted with variable phase shifters, according to section III.A and the Appendix. In a back to back electrical FBMC configuration, subcarriers were included progressively, and the phase shifters in the transmitter were adjusted ensuring a maximum eye opening in the receiver. After these phases had been adjusted, they remained constant and fixed for the whole set of the measurements. The broadband outputs of the IQ mixers were equalized in amplitude with attenuators, multiplexed with a passive combiner, and subsequently amplified. The electrical spectrum at the output of the FBMC transmitter is shown in Fig. 7(b).

The optical link was established with an external cavity laser (ECL) and a polymer based OIQM [47] with a half-wave voltage $V_\pi$=2.5V and a bandwidth of 20 GHz. An optical
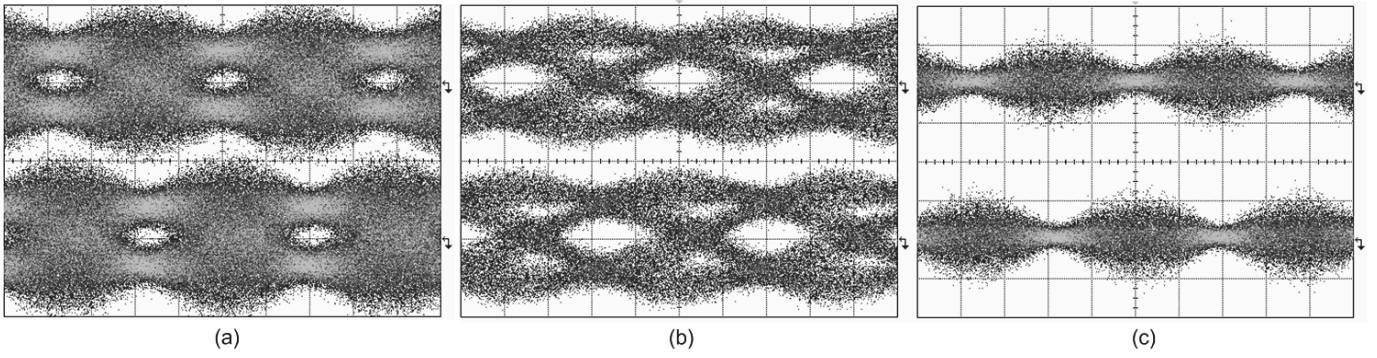
Fig. 8. Received eye diagrams for the I and Q components of the second subchannel, for $P_{IN}$ = -12 dBm, when: (a) three subchannels are transmitted, (b) only the second subchannel is transmitted, and (c) only the first and third subchannels are transmitted. 100 ps per time division.

lower SSB signal was generated, with a sideband suppression ratio of 20 dB, as can be seen in Fig. 7(c). The parallel MZMs inside the OIQM were biased at *quadrature*, and driven by the RF FBMC signal and its HT, with a total rms OMI of ≈20%, or ≈500 $mV_{RMS}$. The carrier to signal power ratio (CSPR) of the optical signal was ≈13 dB. A sensitivity close to -30 dBm for a BER of 3.8·10⁻³ was expected, as explained in section III.C. A higher OMI was avoided, because the peak to peak voltage signal would be higher than the $V_\pi$ value, and more unexpected nonlinear effects could occur in the modulator. The optical signal was transmitted over 1 km of SSMF. At its output, a variable optical attenuator (VOA) was used to emulate more fiber losses. A pre-amplified receiver, consisting of an EDFA and a photo-receiver with a 20 GHz bandwidth, was used at the end of the optical link. The EDFA worked in constant power mode, ensuring 3.5 dBm at its output regardless of the average received optical power, $P_{IN}$. The optical signal was down-converted to its original microwave frequencies, using DD with a single photodiode. The received electrical spectrum is shown in Fig. 7(d).

In the FBMC receiver, the incoming RF signal was amplified, and passively split, before IQ mixers were used to perform the demodulation. The resultant output signals were firstly low pass filtered, removing the LO leakage without influencing the shape of the received baseband pulse. Finally, they were fed to the matched SRRC filters. The LOs of the IQ mixers were locked to the incoming phase of the desired subcarrier, using variable phase shifters that emulated the functionality of a PLL (as described in section III.A). In the received baseband signals, there was an optimum sampling point with minimum ISI and ICI. Final performance was measured in real time with a bit error rate tester (BERT).

Fig. 7(c) shows a gap of 3.5 GHz between the carrier and the signal. These gaps are common in broadband SCM systems as microwave mixers cannot work at low frequencies. In practice, this gap improves the tolerance to second order intermodulation distortions, often referred to as composite second order distortions (CSO), as they fall in low frequencies in DD systems [34]. In the presented scheme, as it can be seen in Fig. 7(d), CSO was low because the OIQM was biased at *quadrature* [36] and the transmission distance was short [34]. As a result, no extra penalty was expected in subchannel 1 due to CSO. On the other hand, CSPR has an important influence in system performance as lower values of CSPR can achieve

better system sensitivity. Carrier suppression can be applied with external filters [8] or directly with the bias of the OIQM [36], but there is a trade-off because in either case it increases CSO [35, 36]. In this experiment, carrier suppression was not applied and CSPR was reduced using a high OMI. With this approach there is also a trade-off between CSPR and nonlinearities [36].

*B. Results*

For a $P_{IN}$=-12 dBm, Fig. 8(a) shows the received eye diagrams for the I and Q components in the second subchannel. This middle subchannel represents the worst case in terms of ICI. Fig. 8 also shows the equivalent diagrams when only the second subchannel is transmitted (b), and when only the first and the third ones are transmitted (c). Neglecting the effects coming from the optical link, the two previous diagrams can be seen as a method to observe the ISI and the ICI that is generated due to the impairments of the microwave components (mainly IQ mixers and orthogonality filters). Despite these impairments, the eye in Fig. 8(a) is still open, allowing for the decoding of the received bits. Fig. 9 shows the average BER of the two components transmitted in every subchannel as a function of $P_{IN}$. Measurements were taken with an optical back to back link, and transmitting over 1 km of SSMF. Considering a hard-decision forward error correction (FEC) code with a 7% overhead, the threshold of acceptable BER is 3.8·10⁻³ [48]. The results show a good
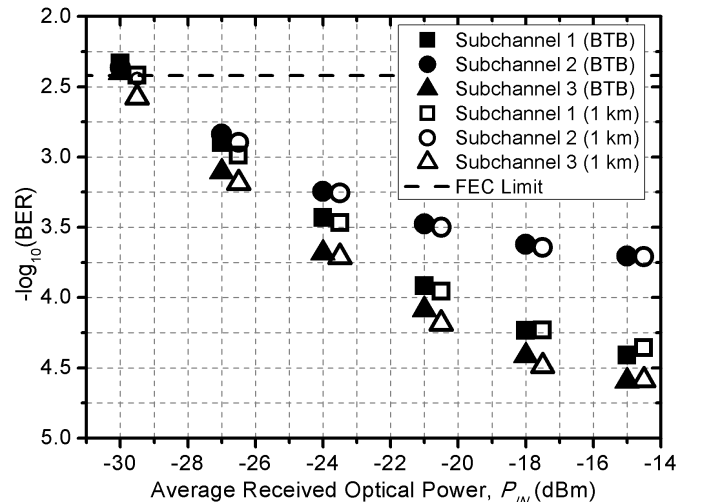


Fig. 9. Average BER as a function of $P_{IN}$ for the I and Q components transmitted in the first, second, and third subchannels for optical back to back (BTB) and transmission over 1 km of SSMF. FEC limit for a 7 % overhead.

agreement with the theoretical predictions. Firstly, the middle subchannel is more impaired than the ones in the extremes, as it can be observed at $P_{IN}$=-14.5 dBm, when the optical noise is low. Secondly, the sensitivity is close to -30 dBm for all the subchannels. When $P_{IN}$ is very low, the optical noise at the output of the EDFA is dominant over the distortion associated with the electrical impairments. Thus, at $P_{IN}$=-30 dBm, the optical noise determines the $Q_F$ of the system. Finally, the dispersion generated by the fiber does not have any influence on the performance. As predicted, OSCM achieves orthogonal transmission without requiring CP. On the other hand, it should be noted that better sensitivities could be achieved by applying carrier suppression in the transmitter, or by applying all-analogue coherent detection like in [49].

The presented results indicate that purely analogue broadband OSCM links are feasible. Neglecting the optical carrier, and assuming that all the multicarrier schemes can be implemented in a SSB configuration, traditional all-analogue SCM/QPSK links achieve a spectral efficiency of 1 bit/s/Hz [5, 7]. In the same conditions, the spectral efficiency of OSCM/QPSK is at least 1.5 bit/s/Hz for a three subchannel configuration, and approaches to 2 bit/s/Hz when a higher number of subchannels is employed. Broadband SCM/16-QAM links have been reported, but DSP has been required to overcome the limitations of the microwave IQ mixers [50]. Radio applications usually employ lower data rate signals, and, as a consequence, the ripple in the group delay of IQ mixers is usually high for broadband electro-optical applications [50]. In that sense, it is noteworthy that the results presented here have been achieved using off-the-shelf IQ mixers and long PRBS sequences of $2^{15}$-1 bits. The spectral efficiency achieved with OSCM/QPSK can be close to the one obtained with SCM/16-QAM, with the advantage of employing a simpler front-end interface in the baseband receiver, a bi-level comparator.

## V. CONCLUSION

SCM allows the implementation of reliable electro-optical transceivers, as it leverages the performance of the more mature microwave components. The main disadvantage of SCM systems is the low spectral efficiency, especially when it is compared with DSP based implementations. The OSCM scheme proposed in this work can potentially double the spectral efficiency of traditional all-analogue SCM links. A real-time all-analogue broadband OSCM system, consisting of three orthogonal 2.7 Gbaud subchannels, has been presented. The use of FBMC schemes with broadband microwave circuits has been discussed and demonstrated. With the appropriate microwave filtering, bits sourced at multi-gigabit rates can be pulse shaped, and modulated and demodulated orthogonally without requiring DSP techniques. Moreover, the combination of FBMC and SCM permits the transmission of orthogonal subchannels over fiber without requiring a CP.

## APPENDIX

This section details a simplified technique to achieve the orthogonal phase alignment in an RF FBMC transmission system, equivalent to the one presented in this work. The original FBMC scheme developed in [27] is shown in Fig. 2, with additional delays and phase shifts included in the signal paths (as described in section III.A). The real physical implementation using IQ mixers, as illustrated in Fig. 7(a), includes extra phase shifts of 180 degrees in some of the LOs, but it can be readily seen that those shifts do not have any influence in the final results. Considering any phase shift between different pairs of baseband data, and any difference in the delay introduced by the IQ mixers at the different RF frequencies, orthogonal phase alignment can be accomplished by adjusting only the phase of the transmitting LOs. This ensures there is a sampling point free of ISI and ICI in the received baseband signals. The required phase shifts in the transmitting LOs will be derived mathematically. In the derivation, a full roll-off $SRRC(\omega)$ extending till $\omega_r$, is used.

Initially, the I component of the $k^{th}$ subchannel is analyzed. As matched $SRRC(\omega)$ filters are used in the transmitter and the receiver, ISI will be zero at $t=nT+dA_k+dB_k$, where $n$ denotes the bit number. The ICI coming from the $(k-1)^{th}$ subchannel can be derived as follows. In the receiver, the interfering spectrum generated by the I component of the $(k-1)^{th}$ subchannel, over the I component of the $k^{th}$ subchannel is:

$$R_{(k-1)I}(\omega) =$$
$$\tfrac{1}{2} SRRC(\omega)\left[ SRRC\left(\omega+\tfrac{2\pi}{T}\right)e^{-j\theta} + SRRC\left(\omega-\tfrac{2\pi}{T}\right)e^{j\theta} \right] (2)$$
$$\cdot e^{j\omega(\tau-\frac{T}{2})}$$

where:

$$\tau = -dA_{k-1} - dB_{k-1}.$$
$$\theta = \pi + \frac{2\pi}{T}dA_{k-1} - \varphi_{k-1} + \omega_k dB_{k-1} + \varphi_k - \omega_k dB_k. \quad (3)$$

As $SRRC(\omega)$ is an even function, the associated temporal signal can be reduced to:

$$r_{(k-1)I}(t) = \tfrac{1}{2\pi}\int_{\frac{-2\pi}{T}}^{\frac{2\pi}{T}} R_{(k-1)I}(\omega)\cdot e^{j\omega t}d\omega =$$
$$\tfrac{1}{2\pi}\int_0^{\frac{2\pi}{T}}\left(\begin{array}{c} SRRC(\omega)\cdot SRRC\left(\omega-\tfrac{2\pi}{T}\right) \\ \cdot \cos\left(\omega\left(t+\tau-\tfrac{T}{2}\right)+\theta\right) \end{array}\right)d\omega. \quad (4)$$

With a change of variable $u = \omega - \pi/T$:

$$r_{(k-1)I}(t) =$$
$$\tfrac{1}{2\pi}\int_{-\frac{\pi}{T}}^{\frac{\pi}{T}}\left(\begin{array}{c} SRRC\left(u+\tfrac{\pi}{T}\right)\cdot SRRC\left(u-\tfrac{\pi}{T}\right) \\ \cdot\cos\left(u\left(t+\tau-\tfrac{T}{2}\right)+\tfrac{\pi}{T}\left(t+\tau-\tfrac{T}{2}+\theta\tfrac{T}{\pi}\right)\right) \end{array}\right)du. \quad (5)$$

When the integrand of eq. (5) is an odd function, the interference cancels. This happens when:

$$t + \tau + \theta \frac{T}{\pi} = nT. \qquad (6)$$

Similarly, in the receiver, the interference generated by the Q component of the $(k-1)^{th}$ subchannel, over the I component of the $k^{th}$ subchannel, can also be deduced. Its associated spectrum is:

$$R_{(k-1)Q}(\omega) =$$
$$-\frac{j}{2} SRRC(\omega) \left[ SRRC(\omega + \tfrac{2\pi}{T})e^{-j\theta} - SRRC(\omega - \tfrac{2\pi}{T})e^{j\theta} \right] (7)$$
$$\cdot e^{j\omega\tau}.$$

Following an equivalent analysis, it can be shown that this ICI also cancels when the conditions presented in eq. (6) are met. In eq. (6), expanding the parameters $\tau$ and $\theta$ (as in eq. (3)), it becomes clear that varying the phase of the $(k-1)^{th}$ subcarrier $\varphi_{k-1}$, the sampling point at which the ICI is equal to zero moves. As it must coincide with the sampling point free of ISI, $t=nT+dA_k+dB_k$, the desired value of $\varphi_{k-1}$ can be derived:

$$\varphi_{k-1} = \varphi_k + \frac{\pi}{T}(dA_{k-1} + dA_k + (2k-1)(dB_{k-1} - dB_k)). \quad (8)$$

With the previous value of phase, the ICI coming from the I component of the $k^{th}$ subchannel, over the I and Q components of the $(k-1)^{th}$ subchannel can also be analyzed yielding the desired results, as it cancels at $t=(2n+1)(T/2)+dA_{k-1}+dB_{k-1}$ and $t=nT+dA_{k-1}+dB_{k-1}$ respectively. Repeating the whole process for the $(k+1)^{th}$ subchannel, it can be obtained that the required value of phase $\varphi_{k+1}$ is:

$$\varphi_{k+1} = \varphi_k + \frac{\pi}{T}(-dA_{k+1} - dA_k + (2k+1)(dB_{k+1} - dB_k)). \quad (9)$$

Due to the symmetry of the system, the same values of $\varphi_{k-1}$ and $\varphi_{k+1}$ are obtained if the Q component of the $k^{th}$ subchannel is analyzed. The functionality of these values was verified by simulation.

It can be concluded that, aligning only the *T/2* shift inside every baseband pair, any number of practical subchannels can be orthogonally aggregated by adjusting the phase shift of every new transmitting LO. This phase moves the time at which the new ICI over the baseband components transmitted in the neighboring subchannels is cancelled, until it coincides with the sampling point, where ISI is also zero. Knowing all the delays of the components, the required phase shifts can be directly introduced in the tracks of a hypothetical integrated circuit or printed circuit board.

REFERENCES

[1] Z. Li, I. Shubin, and X. Zhou, "Optical interconnects: recent advances and future challenges," *Optics Express,* vol. 23, pp. 3717-3720, 2015.
[2] P. Guan, D. Kong, K. M. Roge, H. C. H. Mulvad, M. Galili, and L. K. Oxenlowe, "Real-time all-optical OFDM transmission system based on time-domain optical fourier transformation," in *Proc. OFC*, 2014, p. W4F.1.
[3] H. Masuda, E. Yamazaki, A. Sano, T. Yoshimatsu, T. Kobayashi, E. Yoshida*, et al.*, "13.5-Tb/s (135x111-Gb/s/ch) no-guard-interval coherent OFDM transmission over 6,248 km using SNR maximized second-order DRA in the extended L-band," in *Proc. OFC*, 2009, p. PDPB5.
[4] W. Junyi, X. Chongjin, and P. Zhongqi, "Generation of Spectrally Efficient Nyquist-WDM QPSK Signals Using Digital FIR or FDE Filters at Transmitters," *Lightwave Technology, Journal of,* vol. 30, pp. 3679-3686, 2012.
[5] F. A. Gutierrez, P. Perry, F. Smyth, A. D. Ellis, and L. P. Barry, "Impact of band rejection in multichannel broadband subcarrier multiplexing," *Optical Communications and Networking, IEEE/OSA Journal of,* vol. 7, pp. 248-252, 2015.
[6] R. Olshansky, V. A. Lanzisera, and P. M. Hill, "Subcarrier multiplexed lightwave systems for broad-band distribution," *Lightwave Technology, Journal of,* vol. 7, pp. 1329-1342, 1989.
[7] P. Hill and R. Olshansky, "Bandwidth efficient transmission of 4 Gb/s on two microwave QPSK subcarriers over a 48 km optical link," *Photonics Technology Letters, IEEE,* vol. 2, pp. 510-512, 1990.
[8] R. Hui, Z. Benyuan, H. Renxing, C. T. Allen, K. Demarest, and D. Richards, "Subcarrier multiplexing for high-speed optical transmission," *Lightwave Technology, Journal of,* vol. 20, pp. 417-427, 2002.
[9] B. Charbonnier, S. Menezo, P. O'Brien, A. Lebreton, J. M. Fedeli, and B. Ben Bakir, "Silicon photonics for next generation FDM/FDMA PON," *Optical Communications and Networking, IEEE/OSA Journal of,* vol. 4, pp. A29-A37, 2012.
[10] M. Salter, D. Platt, L. Pettersson, L. Aspemyr, and B. Mingquan, "Circuits and system simulations for 100Gb/s optical SCM transmission," in *Proc. ICECS*, 2009, pp. 960-963.
[11] J. Armstrong, "OFDM for Optical Communications," *Lightwave Technology, Journal of,* vol. 27, pp. 189-204, 2009.
[12] R. Giddings, "Real-time Digital Signal Processing for Optical OFDM-Based Future Optical Access Networks," *Lightwave Technology, Journal of,* vol. 32, pp. 553-570, 2014.
[13] A. Morea, S. Spadaro, O. Rival, J. Perello, F. Agraz, and D. Verchere, "Power management of optoelectronic interfaces for dynamic optical networks," in *Proc. ECOC*, 2011, p. We.8.K.3.
[14] K. P. Benterud, W. A. Krzymien, and W. D. Grover, "Quasi-orthogonal subcarrier multiplexing for high-capacity optical data links," *Electrical and Computer Engineering, Canadian Journal of,* vol. 18, pp. 159-169, 1993.
[15] F. A. Gutierrez, E. P. Martin, P. Perry, A. D. Ellis, P. Anandarajah, F. Smyth*, et al.*, "100 Gbit/s Real-Time All-analogue Filter Bank OFDM based on a Gain-Switched Optical Comb," in *Proc. ECOC*, 2015, p. Th.1.5.4.
[16] N. Cvijetic, "OFDM for short-reach optical networks," in *Proc. IPC*, 2014, pp. 86-86.
[17] *PCI Express Base 2.1 Specification.* Available: https://www.pcisig.com/specifications/pciexpress/base2/#b21
[18] R. Bouziane, P. Milder, R. Koutsoyannis, Y. Benlachtar, C. R. Berger, J. C. Hoe*, et al.*, "Design studies for an ASIC implementation of an optical OFDM transceiver," in *Proc. ECOC*, 2010, p. Tu.5.A.4.
[19] B. Schmidt, A. J. Lowery, and J. Armstrong, "Experimental Demonstrations of Electronic Dispersion Compensation for Long-Haul Transmission Using Direct-Detection Optical OFDM," *Lightwave Technology, Journal of,* vol. 26, pp. 196-203, 2008.
[20] R. P. Giddings, X. Q. Jin, E. Hugues-Salas, E. Giacoumidis, J. L. Wei, and J. M. Tang, "Experimental demonstration of a record high 11.25Gb/s real-time optical OFDM transceiver supporting 25km SMF end-to-end transmission in simple IMDD systems," *Optics Express,* vol. 18, pp. 5541-5555, 2010.
[21] A. Peled and A. Ruiz, "Frequency domain data transmission using reduced computational complexity algorithms," in *Proc. ICASSP*, 1980, pp. 964-967.
[22] I. Dedic, "56Gs/s ADC : Enabling 100GbE," in *Proc. OFC*, 2010, p. OThT6.

[23] I. Orovic, N. Zaric, S. Stankovic, I. Radusinovic, and Z. Veljovic, "Analysis of power consumption in OFDM systems," in *Proc. MIPRO*, 2011, pp. 653-657.

[24] B. Olsson, J. Martensson, and A. Alping, "RF-assisted transmitter and receiver for 100G optical transmission," in *Proc. MWP*, 2011, pp. 180-183.

[25] J. Hubert, "MMIC Design Techniques for Low-Cost High-Volume Commercial Modules," in *Microwave Conference, 2003 33rd European*, 2003, pp. 887-890.

[26] B. Farhang-Boroujeny, "OFDM Versus Filter Bank Multicarrier," *Signal Processing Magazine, IEEE,* vol. 28, pp. 92-112, 2011.

[27] B. Saltzberg, "Performance of an Efficient Parallel Data Transmission System," *Communication Technology, IEEE Transactions on,* vol. 15, pp. 805-811, 1967.

[28] P. Kourtessis and S. D. Walker, "A Complete 8-GHz QPSK-MODEM Featuring Novel Subcarrier and Data Synchronization for Optical Communications," *Communications, IEEE Transactions on,* vol. 55, pp. 987-995, 2007.

[29] I. Seto, H. Shoki, and S. Ohshima, "Optical subcarrier multiplexing transmission for base station with adaptive array antenna," *Microwave Theory and Techniques, IEEE Transactions on,* vol. 49, pp. 2036-2041, 2001.

[30] A. Hilt, A. Zolomy, T. Berceli, G. Jaro, and E. Udvary, "Millimeter Wave Synthesizer Locked To An Optically Transmitted Reference Using Harmonic Mixing," in *Proc. MWP*, 1997, pp. 91-94.

[31] L. Young, "Microwave Filters - 1965," *Microwave Theory and Techniques, IEEE Transactions on,* vol. 13, pp. 489-508, 1965.

[32] G. H. Smith, D. Novak, and Z. Ahmed, "Overcoming chromatic-dispersion effects in fiber-wireless systems incorporating external modulators," *Microwave Theory and Techniques, IEEE Transactions on,* vol. 45, pp. 1410-1415, 1997.

[33] T. Nakatogawa, M. Maeda, and K. Oyamada, "Optical single sideband modulator for distribution of digital broadcasting signals on millimetre-wave band based on self-heterodyne," *Electronics Letters,* vol. 40, pp. 1369-1370, 2004.

[34] W. H. Chen and W. I. Way, "Multichannel single-sideband SCM/DWDM transmission systems," *Lightwave Technology, Journal of,* vol. 22, pp. 1679-1693, 2004.

[35] P. Laurencio, S. O. Simoes, and M. C. R. Medeiros, "Impact of the Combined Effect of RIN and Intermodulation Distortion on OSSB/SCM Systems," *Lightwave Technology, Journal of,* vol. 24, pp. 4250-4262, 2006.

[36] F. A. Gutierrez, P. Perry, F. Smyth, A. D. Ellis, and L. P. Barry, "Optimum Bias Point in Broadband Subcarrier Multiplexing With Optical IQ Modulators," *Lightwave Technology, Journal of,* vol. 33, pp. 258-266, 2015.

[37] B. J. Ainslie and C. R. Day, "A review of single-mode fibers with modified dispersion characteristics," *Lightwave Technology, Journal of,* vol. 4, pp. 967-979, 1986.

[38] J. Maeda, T. Katoh, and S. Ebisawa, "Effect of Fiber Dispersion on Subcarrier QAM Signal in Radio-Over-Fiber Transmission," *Lightwave Technology, Journal of,* vol. 30, pp. 2625-2632, 2012.

[39] T. Fujiwara and K. Kikushima, "140 Carrier, 20GHz SCM Signal Transmission across 200km SMF by Two-step Sideband Suppression Scheme in Optical SSB Modulation," in *Proc. OFC*, 2007, p. OME2.

[40] A. D. Ellis, I. Tomkos, A. K. Mishra, J. Zhao, S. K. Ibrahim, P. Frascella*, et al.*, "Adaptive modulation schemes," in *IEEE/LEOS*, 2009, pp. 141-142.

[41] T. Yan, W. Shieh, and B. S. Krongold, "DFT-Spread OFDM for Fiber Nonlinearity Mitigation," *Photonics Technology Letters, IEEE,* vol. 22, pp. 1250-1252, 2010.

[42] L. B. Du and A. J. Lowery, "Optimizing the subcarrier granularity of coherent optical communications systems," *Optics Express,* vol. 19, pp. 8079-8084, 2011.

[43] P. Poggiolini, Y. Jiang, A. Carena, G. Bosco, and F. Forghieri, "Analytical results on system maximum reach increase through symbol rate optimization," in *Proc. OFC*, 2015, p. Th3D.6.

[44] A. D. Ellis, F. C. G. Gunning, and T. Healy, "Coherent WDM: the achievement of high information spectral density through phase control within the transmitter," in *Proc. OFC*, 2006, p. OThR4.

[45] F. C. G. Gunning, T. Healy, and A. D. Ellis, "Dispersion tolerance of coherent WDM," *Photonics Technology Letters, IEEE,* vol. 18, pp. 1338-1340, 2006.

[46] "Virtex 6 FPGA GTX Transceivers: User Guide.," ed: Xilinx, 2011.

[47] Y. Guomin, E. Miller, J. Mallari, W. Cailin, C. Baoquan, C. Hui*, et al.*, "Small form factor thin film polymer modulators for telecom applications," in *Proc. OFC*, 2012, p. OM3J.1.

[48] "Forward Error Correction for High Bit-Rate DWDM Submarine Systems," *ITU-T Recommendation G.975.1,* 2004.

[49] P. M. Hill and R. Olshansky, "Multigigabit subcarrier multiplexed coherent lightwave system," *Lightwave Technology, Journal of,* vol. 10, pp. 1656-1664, 1992.

[50] B. Olsson, J. Martensson, A. Kristiansson, and A. Alping, "RF-assisted optical dual-carrier 112 Gbit/s polarization-multiplexed 16-QAM transmitter," in *Proc. OFC*, 2010, p. OMK5.